IEEE Access
Multidisciplinary | Rapid Review | Open Access Journal

Received April 13, 2020, accepted May 15, 2020, date of publication May 22, 2020, date of current version June 4, 2020.

Digital Object Identifier 10.1109/ACCESS.2020.2996655

Experimental Study on the Fabrication of 3D Microelectrodes for Electrochemical Micromachining

JIANGUO LEI, BIN XU, AND LIKUAN ZHU

Guangdong Provincial Key Laboratory of Micro/Nano Optomechatronics Engineering, College of Mechatronics and Control Engineering, Shenzhen University, Shenzhen 518060, China

Corresponding author: Likuan Zhu (zhulikuan@szu.edu.cn)

This work was supported in part by the National Natural Science Foundation of China under Grant 51805333, in part by the Science and Technology Innovation Commission Shenzhen under Grant JCYJ20190808143017070, Grant JCYJ20170817094310049, and Grant JSGG20170824111725200, and in part by the Natural Science Foundation of Guangdong Province under Grant 2017A030313309.

ABSTRACT The use of three-dimensional (3D) microelectrodes to machine micro-cavities in electrochemical micromachining (ECMM) can greatly improve processing efficiency. The 3D microelectrodes that are difficult to fabricate by traditional methods can be prepared by laminated object manufacturing and vacuum thermal diffusion bonding (VTDB). However, the VTDB process is very time-consuming, resulting in a long preparation cycle. To solve this problem, the present study proposed an approach combining wire electrochemical micromachining (WECMM) with micro-electric resistance slip welding to fabricate 3D microelectrodes. The machining surface quality and dimensional accuracy of 2D microstructures under different WECMM conditions were investigated. Moreover, the effects of the welding parameters on the bonding quality were studied. The experimental results show that with a 6 V machining voltage, 1.33 μm/s feed rate, and 30 μm movement amplitude for the wire electrode, the machining gap was approximately 10 μm and the machining surface was flat when using a tungsten wire 8 μm in diameter to machine 30 μm thick #304 stainless steel foils by WECMM. Under a 0.3 V welding voltage, 0.2 MPa welding pressure, 20 ms welding time and 160 times slip welding discharge, the error in 3D microelectrodes in lamination direction was smaller than 3 μm. Based on the proposed approach, two typical 3D microelectrodes were successfully fabricated and subsequently applied in ECMM to machine 3D micro-cavities in nickel plates.

INDEX TERMS 3D microelectrode, electrochemical micromachining, welding, 3D micro-cavity.

I. INTRODUCTION

In recent years, with the development of micro-electro-mechanical systems, there has been an increasing demand for microstructures in various fields, such as micro-machinery, micro-electronics, and bio-medical fields, all of which are new challenges for traditional machining method. While electrochemical micromachining (ECMM), as non-traditional, possesses advantage characteristics such as no tool electrode wear, negligible cutting force and capable of machining various microstructures on any electric conductivity materials regardless of the hardness [1], [2]. Additionally, it can avoid defects in the recast layer from electrical discharge machining (EDM), heat-affected zone from laser machining, and residual stress from machining processes. Hence, ECMM has attracted a great amount of attention from researchers.

Wire electrochemical micromachining (WECMM) is one ECMM technique. As such a promising micromachining technique, it can machine complex planar contour microstructures. Zhu *et al.* [3] used an in situ fabricated wire electrode with a diameter of 5 μm to process microstructures by WECMM. Applying an ultrashort voltage pulse, Shin *et al.* [4] machined micro-grooves and micro-gears into stainless steel plates using a Ø 10 μm wire as a tool electrode, significantly reducing the machining gap. To enhance mass transport, Xu *et al.* [5] utilized cathode travelling and anode vibration in WECMM and successfully fabricated micro-cams on a cobalt-based superalloy, improving the machining surface roughness (R_a = 0.058 μm, R_{max} = 0.670 μm). To enhance electrolyte renewal and bubble removal,

The associate editor coordinating the review of this manuscript and approving it for publication was Sanket Goel.

Fang *et al.* [6] introduced a large-amplitude vibration of a ribbed wire electrode in WECMM, significantly improving the material removal rate and machining efficiency. To improve machining efficiency and homogeneity, Meng *et al.* [7] introduced a carbon nanotube fiber (CNF) electrode in WECMM for complex-shaped microstructure fabrication of metallic glass. The CNF electrode, with a series of surface micro textures and high surface hydrophilicity, enhanced the mass transport in the machining gap.

With regard to the ECMM of 3D micro-cavities, a layer-by-layer scanning machining strategy with a micro cylindrical electrode is usually utilized. The microelectrode looks like a miniature milling cutter in the machining process. Based on the finite time constant for double-layer charging and the application of an ultrashort voltage pulse, Schuster [8] machined a delicate Cu prism (cross-section, 5 μm by 10 μm; height, 12 μm) and a Cu tongue (2.5 μm by 10 μm by 15 μm) into a Cu sheet by scanning a Ø 10 μm cylindrical Pt wire in ECMM. Kock *et al.* [9] machined a spiral trough with a depth of 5 μm and a triangular trough with a depth of 1 μm into Ni sheets by scanning ECMM with a tungsten cylindrical electrode. To reduce the taper of 3D micro-cavities, Kim *et al.* [10] introduced a disc-like electrode into ECMM and fabricated various 3D microstructures. The stray corrosion on the sidewalls of microstructures was greatly reduced. Ghoshal and Bhattacharyya [11] established simulation models of different shaped microelectrodes in ECMM and performed the corresponding experiments. These researchers found that reversed taper microelectrodes could significantly reduce the taper angle of microstructures. To improve the machining accuracy of microstructures, Liu *et al.* [12] established a mathematical model for micro electrochemical milling by layers and successfully fabricated 3D complex microstructures with physical dimensions of several tens of microns using in situ fabricated cylindrical electrodes. Kurita *et al.* [13] machined 3D shapes by scanning the prismatic electrode with a 200 μm square in ECMM. To improve the surface quality and mechanical property of 3D microstructures, Zeng *et al.* [14] performed micro electrochemical milling with a 0.1 mm in diameter tungsten rod electrode to remove recast layer and surface defects of 3D microstructures machined by EDM. Nguyen *et al.* [15] utilized low-resistivity deionized water as a working fluid in micro-ED/EC milling with a tungsten electrode of diameter 100 μm, significantly improving surface integrity and dimensional accuracy of 3D microstructures.

To improve the anti-interference ability of the microelectrode, the use of a laminated 3D microelectrode was an excellent candidate method [16]. Xu *et al.* [17], [18] combined wire electrical discharge machining (WEDM) with vacuum thermal diffusion bonding to prepare a laminated 3D microelectrode and subsequently used it to machine 3D micro-cavities by ECMM. Wu *et al.* [19] proposed vibration-assisted ECMM combined with polishing to machine 3D micro-cavities by using a laminated 3D microelectrode and an electrolyte with suspended B_4C particles, improving the machining efficiency and surface quality of the micro-cavities. The abovementioned 3D microelectrodes could be obtained through WEDM combined with vacuum thermal diffusion bonding. However, the vacuum thermal diffusion bonding process was time-consuming and the thermal diffusion time took approximately 10 h. If with the heating and cooling time included, preparation of the laminated 3D microelectrode would need around 50 h. In addition, due to the large diameter (approximately 180 μm) of the wire in WEDM, the dimensions of the machined micro-features were hundreds of micrometers.

To shorten the preparation time of 3D microelectrodes and obtain microelectrodes with micro-feature dimensions smaller than 180 μm, this paper proposed an approach combining WECMM with micro-electric resistance slip welding (micro-ERSW) to fabricate 3D microelectrodes for ECMM. The experimental method, setup and materials are presented in section II. Section III illustrates an investigation to determine the proper parameters for WECMM, such as machining voltage, feed rate of the wire electrode and movement amplitude of the wire electrode. Section IV shows an investigation to determine the suitable welding parameters for micro-ERSW. In section V, based on the optimal parameters, 3D microelectrodes are fabricated and subsequently applied in ECMM to machine 3D micro-cavities. Finally, conclusions of this research are drawn.

II. EXPERIMENTAL

A. METHODS

Fig. 1 shows the process of fabricating 3D microelectrodes, and three key steps are described as follows:

(1) CAD modeling and preprocessing. Based on a 3D micro-cavity model, a 3D microelectrode model was prepared (Fig. 1a). Then, the 3D microelectrode model was sliced into several thin cross-sectional layers in a given direction by slicing software (Fig. 1b). Subsequently, the total number of sliced layers and the profile data of each 2D cross-sectional layer were obtained.

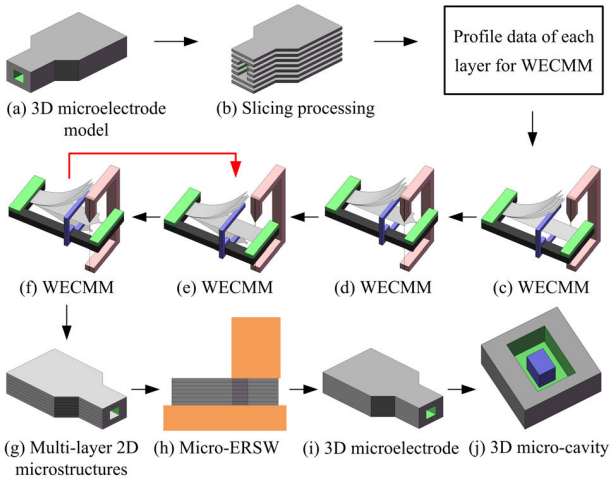

FIGURE 1. Process of 3D microelectrode fabrication.

(2) WECMM. According to the profile data of all the layers, stainless steel foils were cut by WECMM to obtain multi-layer 2D microstructures. First, one end of the multi-layer stainless steel foils was bonded by resistance spot welding and fixed on a fixture. Then, the other end of the first layer was fixed on the fixture by a magnet to keep the layer straight. Next, the other layers of the stainless steel foils were elastically bent upward with a stopper for WECMM (Fig. 1c). The first layer was cut (Fig. 1d) and then bent downward with the stopper, and the former upper end of the second layer was fixed on the fixture for WECMM (Fig. 1e). By repeating these steps (Fig. 1e-f), multi-layer 2D microstructures were obtained (Fig. 1g).

(3) Micro-ERSW. To improve bonding quality, the obtained multi-layer 2D microstructures were first immersed in ethanol and subjected to ultrasonic vibration. After cleaning, the multi-layer 2D microstructures were placed on a Cu plate electrode and then lightly pressed by a Cu bar electrode on the upper surface for micro-ERSW. As a result, the 3D micro-electrode was obtained (Fig. 1h-i). Finally, the microelectrode was applied in ECMM to process 3D micro-cavities (Fig. 1j).

Fig. 2 shows the principle of WECMM. According to the programmed machining path, the wire electrode moved towards the workpiece (anode) at a constant speed, and the wire electrode moved up and down periodically along the axis direction of itself. The workpiece was machined by means of an electrochemical reaction. To avoid deformation of the wire electrode caused by the electrolyte flow, a stream of electrolyte coaxial with the wire electrode was used [20], as shown in Fig. 2. During processing, the axially vibrating wire electrode reciprocating moved up and down at a speed of 2 mm/min, which was helpful to enhance the removal of obsolete electrolyte and electrolytic products from the machining gap and improve machining stability as well as quality.

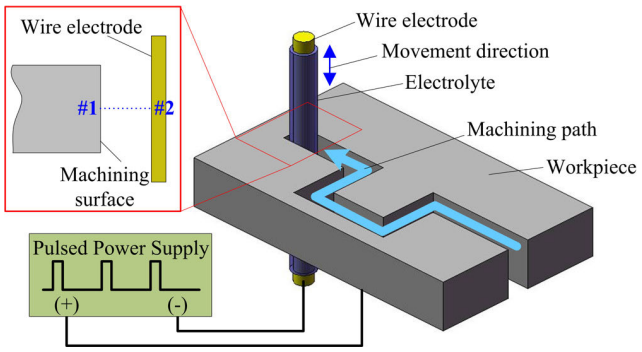

FIGURE 2. Principle of WECMM with a reciprocating travelling of the wire electrode.

A schematic diagram of micro-ERSW is shown in Fig. 3. The Cu bar electrode and Cu plate electrode were connected to the two poles of the welding power. When the Cu bar electrode was pressed on the surface of the stainless steel foil, a current was produced in the loop consisting of the welding power, the Cu bar electrode, the multi-layer stainless steel foils and the Cu plate electrode. Then, the multi-layer stainless steel foils were bonded by resistance heat.

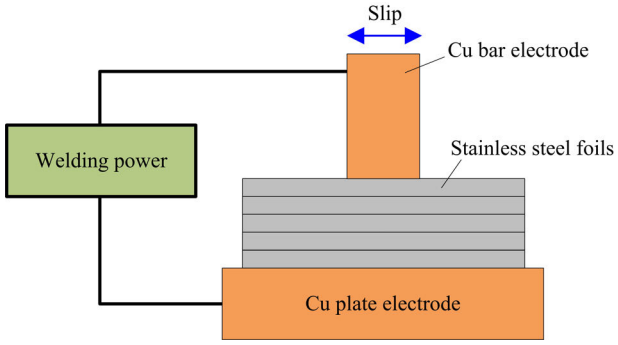

FIGURE 3. Schematic diagram of micro-ERSW.

B. EXPERIMENTAL SETUP AND MATERIALS

A three-axis PI high precision motion platform (model: M511.DD, motion accuracy: 0.2 μm), produced by German PI company, was chosen to control the machining path and axial reciprocating movement of the wire electrode. An oscilloscope was used to monitor the pulsed signal in real time in the machining process. A pulsed power supply was utilized to produce ultrashort pulses. An inverter DC resistance welding machine (model: UF25B), produced by Shenzhen Will-Best Welding Equipment Co., Ltd., was used for the micro-ERSW to bond the multi-layer stainless steel foil 2D microstructures. A scanning electron microscope (model: S-3400N), manufactured by the Hitachi company from Japan, was used to observe the surface morphology of the 3D microelectrodes and microstructures. A laser scanning confocal microscope (model: VK-X200K) manufactured by the Japan KEYENCE Company was used to measure the profile of 3D micro-cavities.

Foils of 304 stainless steel 30 μm in thickness, manufactured by the German Pincog Company, were used to fabricate 3D microelectrodes for ECMM. The wire electrode was a tungsten wire with a diameter of 8 μm. Nickel plates were selected as the workpiece to machine 3D micro-cavities by ECMM using the prefabricated 3D microelectrodes. The electrolyte used in the WECMM process and ECMM process comprised deionized water and sodium nitrate ($NaNO_3$) at a concentration of 1.25 g/L and a pH of 7.1.

III. WECMM OF STAINLESS STEEL 2D MICROSTRUCTURES

The multi-layer 2D microstructures obtained by WECMM were stacked and bonded to form 3D microelectrodes. Therefore, the quality of the 2D microstructures, including the surface quality and machining gap, had a great influence on the quality of the 3D microelectrodes. The machining gap was an important index to evaluate the machining accuracy of the 2D microstructures. To improve the machining quality of the 2D microstructures, the process parameters (machining voltage, feed rate and movement amplitude of wire electrode) were investigated in detail.

A. MACHINING VOLTAGE

To obtain the optimal machining voltage, this experiment utilized different machining voltages to cut stainless steel foils. The process parameters were described as follows: a feed rate of 1.33 μm/s, a movement amplitude of 30 μm, and a machining voltage ranging from 5 V to 9 V.

The influence of the machining voltage on the machining gap is illustrated in Fig. 4a. Using COMSOL 5.2, the current densities on the machining surface of the workpiece with different machining voltages were obtained, as shown in Fig. 4b. When the voltage was 5 V, the electrochemical dissolution on the workpiece became difficult due to the low current density, resulting in frequent electric short circuiting. The machined surface became uneven, and the machining gap was large. When the voltage increased from 5 V to 6 V, the current density increased (Fig. 4b), and the machining process stabilized. As a result, the machined surfaces were even, and the machining gap decreased to approximately 10 μm. However, the machining precision decreased when the voltage varied from 6 V to 9 V, which indicated that the material removal volume at the same point increased due to the excessively high current density.

B. FEED RATE OF THE WIRE ELECTRODE

Feed rate of the wire electrode greatly affected the machining stability, further influenced the machining accuracy. To determine suitable feed rate, with a machining voltage of 6 V and a movement amplitude of 30 μm, different feed rates ranging from 0.33 μm/s to 1.67 μm/s were investigated in WECMM. The effect of the feed rate on the machining gap is shown in Fig. 5a. When the feed rate was 0.33 μm/s, the machined surface was flat, but the machining gap was large. As the feed rate increased to 1.33 μm/s, the processing time at the same position decreased, and the material removal volume was reduced. Therefore, the machining gap decreased, and the machining accuracy was improved. Additionally, the machining process was extraordinarily stable. The black curve in Fig. 5b shows the machining current during fabrication. However, when the feed rate was too fast (1.67 μm/s), the workpiece material could not be removed quickly, resulting in frequent electric short circuit and extremely unstable machining current during machining, as the red curve shows in Fig. 5b. As a result, the distribution of the electric field in the subsequent machining gap was greatly affected, and even the machined path (S_1) deviated from the programmed

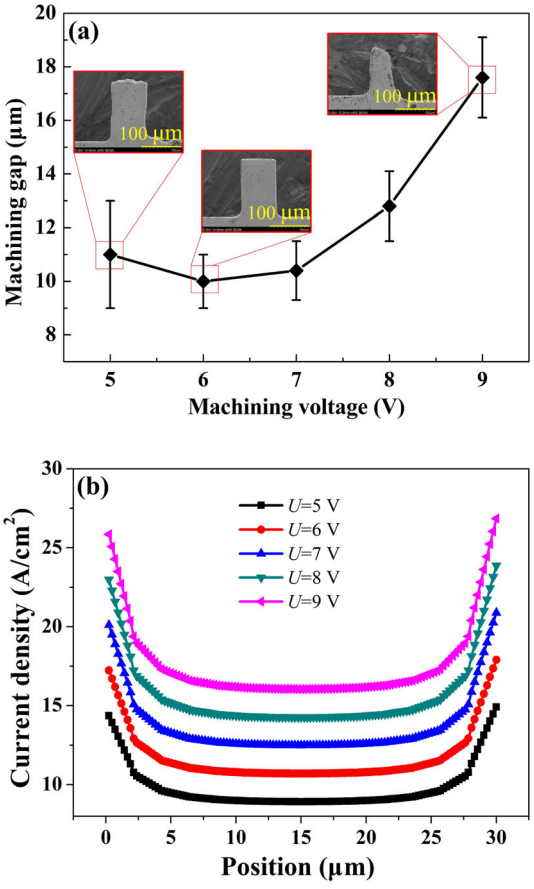

FIGURE 4. (a) Effect of machining voltage on machining gap. (b) Current density of machining surface of workpiece with different voltages.

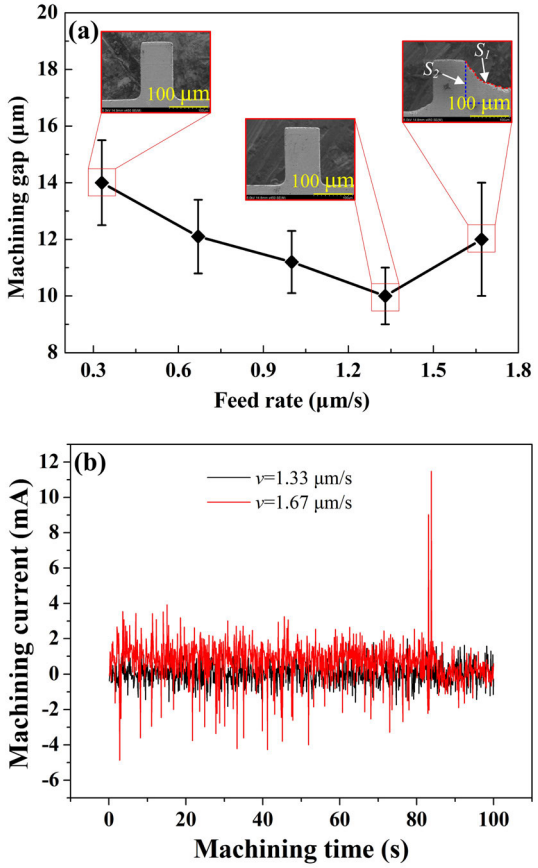

FIGURE 5. (a) Effect of feed rate on machining gap. (b) Machining current with different feed rates.

path (S_2), as shown in Fig. 5a. Thus, the feed rate was optimized at 1.33 μm/s in the experiment.

C. MOVEMENT AMPLITUDE OF THE WIRE ELECTRODE

To improve the machining accuracy of WECMM, the wire electrode movement amplitude was investigated. At a machining voltage of 6 V and a feed rate of 1.33 μm/s, the influence of the movement amplitude of the wire electrode ranging from 10 μm to 50 μm on the machining gap is shown in Fig. 6a. The velocity distribution from point #1 on the machining surface of the workpiece to point #2 on the wire electrode (Fig. 2) in the machining gap with different movement amplitudes is presented in Fig. 6b.

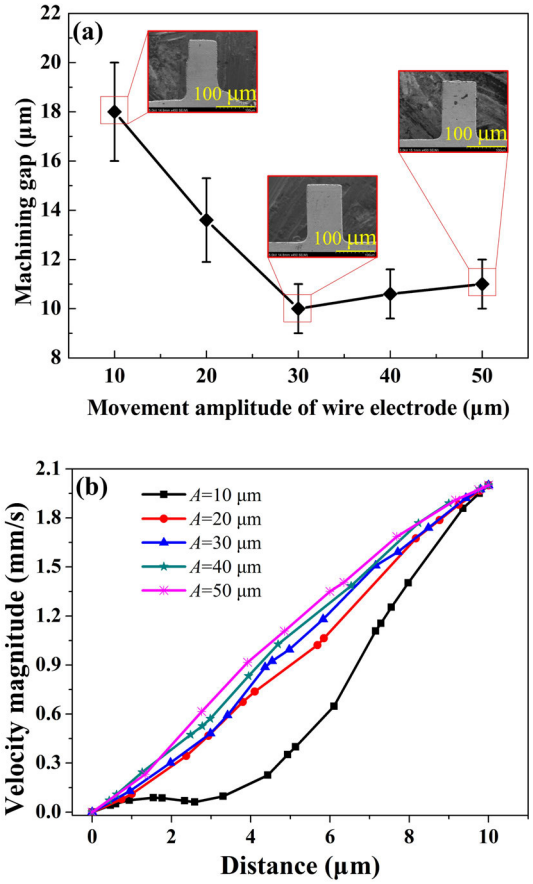

FIGURE 6. (a) Effect of movement amplitude of wire electrode on machining gap. (b) Velocity magnitude from machining surface of workpiece to wire electrode in the machining gap with different movement amplitudes.

Fig. 6a and b shows that with increasing movement amplitude, the machining gap initially decreased and then increased slightly, and the velocity of the electrolyte near the machining surface of the workpiece increased gradually. The experiment was carried out with a movement amplitude of 10 μm, and the velocity of the electrolyte near the machining surface was extremely small, leading to electrolyte renewal becoming extraordinarily difficult. Consequently, the machining process was unstable. When the movement amplitude increased to 30 μm, the velocity of the electrolyte near the machining surface increased, which was beneficial for renewing the electrolyte and removing electrolytic products in the machining gap. The machining stability and accuracy were improved. However, when the movement amplitude was larger than 30 μm, the machining gap increased slightly, which may be the result of either the inhomogeneity of the wire electrode or insufficient verticality between the wire electrode and the workpiece [4].

IV. MICRO-ERSW OF STAINLESS STEEL FOILS

Micro-ERSW was a key preparation for 3D microelectrodes and determines the quality of 3D microelectrodes. Therefore, choosing effective welding parameters, such as the welding voltage, pressure and time, was beneficial for improving the bonding quality between the 2D microstructures and avoiding the formation of nuggets and plastic deformation of the 2D microstructures.

A. WELDING VOLTAGE

Welding voltage applied to the bar copper electrode and plate copper electrode was one of the decisive elements of the quality of the welding zone. To obtained proper welding voltage, the experiments were carried out with various voltage options. Machining conditions for this set of experiments were as follows: a welding pressure of 0.2 MPa, a single welding time of 20 ms, and welding voltage ranging from 0.2 V to 0.4 V.

A low voltage (0.2 V) resulted in insufficient resistance heat in the welding zone and was followed by poor bonding between the stainless steel foils or even no bonding at all (Fig. 7a), while when the voltage was increased to 0.3 V, under the action of sufficient resistance heat, the bonding quality was greatly improved. The cross-section metallographic image (Fig. 7b) shows that the bonding quality of the welding zone was greatly improved; although bonding interfaces still existed, there were no gaps. The bonding interfaces had no influence on the machining of 3D micro-cavities by ECMM. However, if the voltage was raised to 0.4 V, due to

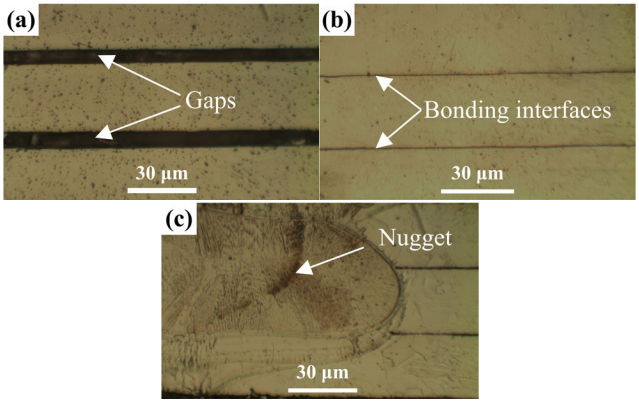

FIGURE 7. Cross-section metallographic images of the welding zone with different welding voltages: (a) 0.2 V. (b) 0.3 V. (c) 0.4 V.

excessive resistance heat, nuggets formed in the welding zone (Fig. 7c), and consequently, plastic deformation of the stainless steel foils occurred. Therefore, to ensure good welding quality for 3D microelectrodes, a welding voltage of 0.3 V was chosen.

B. WELDING PRESSURE

The contact resistance in the welding zone was determined by the welding pressure. From the microcosmic perspective, all the surfaces of the conductors were uneven. When two layers of stainless steel foils were stacked together, physical contact occurred only at the convex points, which greatly decreased the contact area. The total resistance was higher than the sum of the resistances of two stainless steel foils, and the balance value was called the contact resistance. Machining conditions for this set of experiments were as follows: a welding voltage of 0.3 V, a single welding time of 20 ms, and welding voltage ranging from 0.1 MPa to 0.3 MPa.

The resistance of the welding zone consisted of the stainless steel foil resistance and contact resistance. If the welding pressure was too low, the contact resistance was comparatively high and when a current passed through the welding zone, sparks splashed and the stainless steel foils even fractured (Fig. 8a). An appropriate increase in the welding pressure resulted in close contact between the stainless steel foils, increased the contact area and decreased the resistance in the welding zone, avoiding spark splashes. However, if the welding pressure was too high, the stainless steel foils plastically deformed, reducing the quality of the 3D microelectrodes. Therefore, to avoid spark splashes and plastic deformation of stainless steel foils, after the experiments, 0.2 MPa was chosen as the optimum welding pressure.

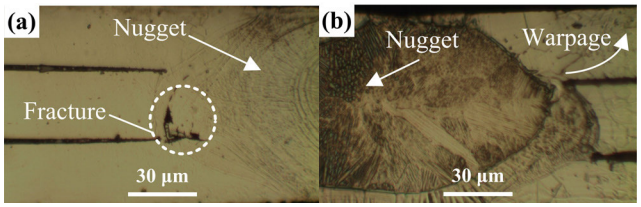

FIGURE 8. (a) Fracture of stainless steel foils caused by spark splashes. (b) Warpage deformation of the stainless steel foils due to excessive welding pressure.

C. WELDING TIME

According to the law of joule heat, the resistance heat (Q) of the welding zone can be expressed by:

$$Q = \int_0^t i^2(t)R(t)dt \tag{1}$$

where, t is the welding time, $i(t)$ is the instantaneous current of the welding zone, and $R(t)$ is the instantaneous resistance of the welding zone.

Eq. (1) shows that as the welding time increased, the resistance heat in the welding zone increased. To study the influence of the welding time on the welding quality, experiments were carried out by varying the welding time while the other parameters were held constant. The slip welding discharge was set at 160 times with a single welding time of 10 ms. However, 10 ms was too short, and insufficient resistance heat was generated in the welding zone, leading to small gaps (Fig. 9a) between the stainless steel foils. When the single welding time was increased to 20 ms, the accumulated resistance heat eliminated the gaps between the stainless steel foils. However, when the single welding time continued to increase to 30 ms, the overaccumulation of resistance heat resulted in nugget formation in the welding zone (Fig. 9b). The longer the welding time was, the more easily nuggets formed. To improve the bonding quality of the stainless steel foils, the optimal single welding time was 20 ms (Fig. 7b).

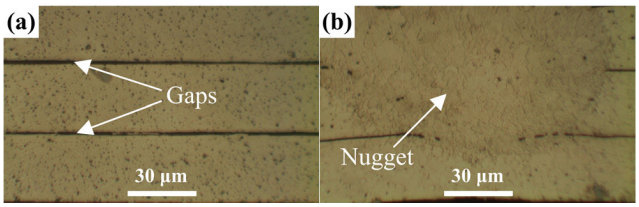

FIGURE 9. Cross-section metallographic images of the welding zone with different single welding time: (a) 10 ms. (b) 30 ms.

V. FABRICATION AND APPLICATION OF 3D MICROELECTRODES

To verify the feasibility of the use of 3D microelectrodes in machining 3D micro-cavities, two typical 3D microelectrodes were fabricated. The 3D CAD models of the microelectrodes are shown in Fig. 10a and b.

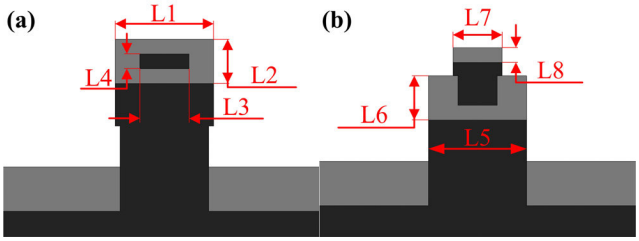

FIGURE 10. CAD models of the 3D microelectrodes.

First, 30-μm-thick multi-layer stainless steel foils were cut by WECMM using the optimized process parameters to obtain multi-layer 2D microstructures. The optimal process parameters were as follows: a machining voltage of 6 V, a feed rate of 1.33 μm/s and a movement amplitude of 30 μm. Then, using the optimal welding parameters, a 0.3 V welding voltage, a 0.2 MPa welding pressure and 160 times slip welding discharge with a single welding time of 20 ms, the multi-layer 2D microstructures were laminated and bonded by micro-ERSW to form 3D microelectrodes (Fig. 11a and d). The time to fabricate a 3D microelectrode was approximately 2 h, including WECMM and micro-ERSW. Compared with the combination of WEDM and thermal diffusion bonding, the preparation efficiency of 3D microelectrodes was

improved by 96%. Finally, under the action of a 10 V machining voltage, 80 ns pulse duration and 160 ns pulse interval, the 3D microelectrodes were used for ECMM with an up-and-down reciprocating processing strategy, and 3D micro-cavities were machined into nickel plates (Fig. 11b and e). Fig. 11c shows the profile of the 3D micro-cavity in Fig. 11b along the L3' direction, and Fig. 11f shows the profile of the 3D micro-cavity in Fig. 11e along the L7' direction.

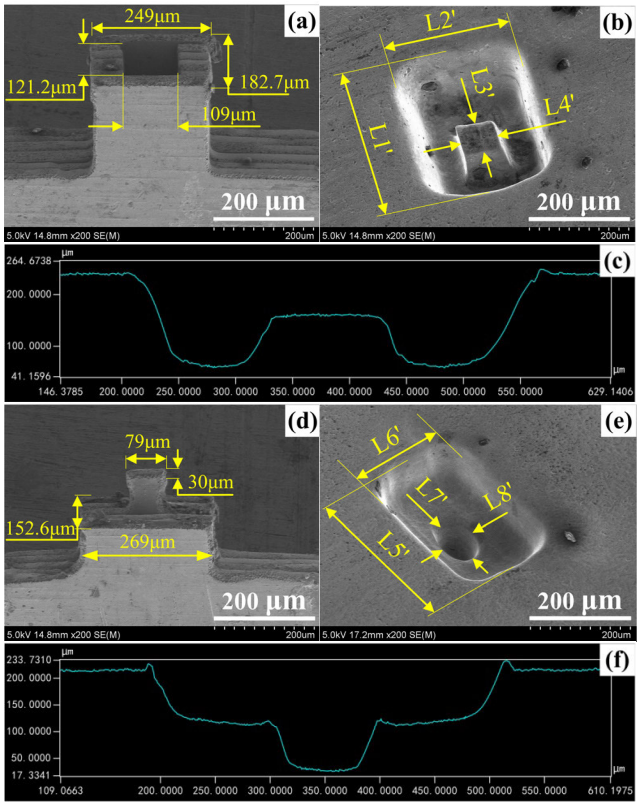

FIGURE 11. (a), (d) 3D microelectrodes. (b), (e) 3D micro-cavities machined by ECMM. (c), (f) Profiles of 3D micro-cavities in (b) and (e), respectively.

Table 1 shows the dimensional values of the fabricated 3D microelectrodes and the machined 3D micro-cavities. Compared with the CAD models, the dimensional errors of the 3D microelectrodes were smaller than 3 μm. The sidewalls of the micro-cavity were always under electrochemical dissolution during machining; therefore, the 3D micro-cavity had a bell mouth. As a result, the dimension at the entrance of the machined 3D micro-cavities was much larger than the dimension of the 3D microelectrodes.

TABLE 1. Dimensional values of the fabricated 3D microelectrodes and the machined 3D micro-cavities shown in Figs. 10 and 11.

Dimensional symbols	Dimensional values (μm)		Dimensional symbols	Dimensional values (μm)
	CAD models	Fabricated 3D microelectrodes		Machined 3D micro-cavities
L1	250	249	L1'	351
L2	180	182.7	L2'	289
L3	110	109	L3'	91
L4	120	121.2	L4'	97
L5	270	269	L5'	314
L6	150	152.6	L6'	220
L7	80	79	L7'	92
L8	30	30	L8'	68

VI. CONCLUSIONS

A method combining WECMM and micro-ERSW was proposed to fabricate 3D microelectrodes, significantly reducing the preparation cycle, and 3D micro-cavities were processed by ECMM with the fabricated 3D microelectrodes. The optimal process parameters of WECMM and micro-ERSW were obtained. According to the experimental results, the main conclusions are summarized as follows:

1) The optimal process parameters of WECMM were a machining voltage of 6 V, a feed rate of 1.33 μm/s and a movement amplitude of 30 μm. With the parameters described above, the machining process was stable, and the flow velocity distribution helped to remove electrolytic products and renew the electrolyte in the machining gap. A machining gap with a width of approximately 10 μm was obtained, and the machining surface was uniform.

2) The up-and-down reciprocating movement of the wire electrode was helpful for removing electrolytic products from the machining gap and renewing the electrolyte to guarantee more stable machining.

3) With a 0.3 V welding voltage, a 0.2 MPa welding pressure and 160 times slip welding discharge with a single welding time of 20 ms, a good bonding quality between stainless steel foils was obtained by micro-ERSW. There were no gaps, nuggets or plastic deformation in the welding zone.

4) 3D microelectrodes with micro-feature dimensions smaller than 180 μm were successfully obtained by combining WECMM and micro-ERSW. The production time for one 3D microelectrode was approximately 2 h, and the preparation efficiency of the 3D microelectrode was improved by 96% compared with the combination of WEDM and vacuum thermal diffusion bonding. In addition, 3D micro-cavities were machined into nickel plates through ECMM using the 3D microelectrodes.

REFERENCES

[1] S. H. Ryu, "Eco-friendly ECM in citric acid electrolyte with microwire and microfoil electrodes," *Int. J. Precis. Eng. Manuf.*, vol. 16, no. 2, pp. 233–239, Feb. 2015.

[2] W. Natsu, H. Nakayama, and Z. Yu, "Improvement of ECM characteristics by applying ultrasonic vibration," *Int. J. Precis. Eng. Manuf.*, vol. 13, no. 7, pp. 1131–1136, Jul. 2012.

[3] D. Zhu, K. Wang, and N. S. Qu, "Micro wire electrochemical cutting by using *in situ* fabricated wire electrode," *CIRP Ann.-Manuf. Technol.*, vol. 56, no. 1, pp. 241–244, 2007.

[4] H. S. Shin, B. H. Kim, and C. N. Chu, "Analysis of the side gap resulting from micro electrochemical machining with a tungsten wire and ultrashort voltage pulses," *J. Micromech. Microeng.*, vol. 18, no. 7, pp. 1–7, Jul. 2008.

[5] K. Xu, Y. Zeng, P. Li, and D. Zhu, "Study of surface roughness in wire electrochemical micro machining," *J. Mater. Process. Technol.*, vol. 222, pp. 103–109, Aug. 2015.

[6] X. L. Fang, X. H. Zou, M. Chen, and D. Zhu, "Study on wire electrochemical machining assisted with large-amplitude vibrations of ribbed wire electrodes," *CIRP Ann.-Manuf. Technol.*, vol. 66, no. 1, pp. 205–208, 2017.
[7] L. Meng, Y. Zeng, X. Fang, and D. Zhu, "Wire electrochemical micromachining of metallic glass using a carbon nanotube fiber electrode," *J. Alloys Compounds*, vol. 709, pp. 760–771, Jun. 2017.
[8] R. Schuster, V. Kirchner, P. Allongue, and G. Ertl, "Electrochemical micromachining," *Science*, vol. 289, no. 5476, pp. 98–101, Jul. 2000.
[9] M. Kock, V. Kirchner, and R. Schuster, "Electrochemical micromachining with ultrashort voltage pulses–a versatile method with lithographical precision," *Electrochimica Acta*, vol. 48, nos. 20–22, pp. 3213–3219, Sep. 2003.
[10] B. H. Kim, S. H. Ryu, D. K. Choi, and C. N. Chu, "Micro electrochemical milling," *J. Micromech. Microeng.*, vol. 15, no. 1, pp. 124–129, Jan. 2005.
[11] B. Ghoshal and B. Bhattacharyya, "Investigation on profile of microchannel generated by electrochemical micromachining," *J. Mater. Process. Technol.*, vol. 222, pp. 410–421, Aug. 2015.
[12] Y. Liu, D. Zhu, and L. Zhu, "Micro electrochemical milling of complex structures by using *in situ* fabricated cylindrical electrode," *Int. J. Adv. Manuf. Technol.*, vol. 60, nos. 9–12, pp. 977–984, Jun. 2012.
[13] T. Kurita, K. Chikamori, S. Kubota, and M. Hattori, "A study of three-dimensional shape machining with an ECμM system," *Int. J. Mach. Tools Manuf.*, vol. 46, nos. 12–13, pp. 1311–1318, Oct. 2006.
[14] Z. Zeng, Y. Wang, Z. Wang, D. Shan, and X. He, "A study of micro-EDM and micro-ECM combined milling for 3D metallic micro-structures," *Precis. Eng.*, vol. 36, no. 3, pp. 500–509, Jul. 2012.
[15] M. D. Nguyen, M. Rahman, and Y. S. Wong, "Enhanced surface integrity and dimensional accuracy by simultaneous micro-ED/EC milling," *CIRP Ann.-Manuf. Technol.*, vol. 61, no. 1, pp. 191–194, 2012.
[16] J. Lei, X. Wu, B. Wu, B. Xu, D. Guo, and J. Zhong, "Fabrication of 3D microelectrodes by combining wire electrochemical micromachining and micro-electric resistance slip welding," *Procedia CIRP*, vol. 42, pp. 825–830, Apr. 2016.
[17] B. Xu, X.-Y. Wu, J.-G. Lei, X. Liang, H. Zhao, D.-J. Guo, and S.-C. Ruan, "Micro-ECM of 3D micro-electrode for efficiently processing 3D microstructure," *Int. J. Adv. Manuf. Technol.*, vol. 91, nos. 1–4, pp. 709–717, Jul. 2017.
[18] B. Xu, X.-Y. Wu, J.-G. Lei, R. Cheng, S.-C. Ruan, and Z.-L. Wang, "Laminated fabrication of 3D micro-electrode based on WEDM and thermal diffusion welding," *J. Mater. Process. Technol.*, vol. 221, pp. 56–65, Jul. 2015.
[19] Z.-Z. Wu, X.-Y. Wu, J.-G. Lei, B. Xu, K. Jiang, J.-M. Zhong, D.-F. Diao, and S.-C. Ruan, "Vibration-assisted micro-ECM combined with polishing to machine 3D microcavities by using an electrolyte with suspended B4C particles," *J. Mater. Process. Technol.*, vol. 255, pp. 275–284, May 2018.
[20] Y.-B. Zeng, Q. Yu, S.-H. Wang, and D. Zhu, "Enhancement of mass transport in micro wire electrochemical machining," *CIRP Ann.-Manuf. Technol.*, vol. 61, no. 1, pp. 195–198, 2012.

JIANGUO LEI received the M.Eng. degree in mechanical engineering and the Ph.D. degree in optical engineering from Shenzhen University, Shenzhen, China, in 2012 and 2016, respectively. He is currently an Assistant Professor with Shenzhen University. He has published more than ten research articles. His research interests include electrochemical micromachining and micro electrical discharge machining.

BIN XU received the M.Eng. degree in mechanical engineering and the Ph.D. degree in optical engineering from Shenzhen University, Shenzhen, China, in 2010 and 2013, respectively. He is currently an Associate Professor with Shenzhen University. His research interests include laser machining and microfabrication technique.

LIKUAN ZHU received the M.Eng. degree and the Ph.D. degree in mechanical engineering from the Harbin Institute of Technology, Harbin, China, in 2011 and 2018, respectively. He is currently an Assistant Professor with Shenzhen University, Shenzhen, China. His research interests include flow fluent analysis and microfabrication technique.